Satellight
Commission of the European Communities

DNMI

Fourth SATELLIGHT meeting, Oldenburg June 5 - 6 1997

HORIZONTAL AND VERTICAL ILLUMINANCE/IRRADIANCE FROM 4 IDMP STATIONS

by

Jan Asle Olseth and Arvid Skartveit

SATELLIGHT Programme JOR3-CT950041
First draft, June 1997

1. INTRODUCTION

Most radiation-driven processes are spectrally selective, like the photosynthesis or the erythemal response of human skin to ultraviolet radiation. Equally well-known is the concept of daylight, i.e. solar radiation evaluated in proportion to its capability of stimulating the human eye. Even though daylight data are in great demand, they frequently have to be estimated from prescribed luminous efficacies and observed or estimated beam and diffuse irradiance.

The present note deals with observed and modelled relationships between irradiance and illuminance measured on horizontal and vertical surfaces at the four IDMP stations Gävle, Geneva, Lyon and Lisboa.

2. DATA

2.1 Meteosat/Heliosat data

The Heliosat procedure is described by Beyer et al. (1996). A measure of cloud cover is inferred from pixel counts in the VIS-channel (0.5 - 0.9 μm), and this measure is subsequently used to estimate surface global irradiance as a fraction of the irradiance under clear sky conditions. This procedure is carried out with a choice of alternative clear sky models, viz. Heliosat Versions 2n, and 3n (Hammer 1997; Kasten/Dumortier with Linke turbidity factor 3 [2n] and monthly factors [3n]), and for a modification of Version 2n proposed by Ineichen (1997) on basis on Geneva data. Global radiation data for 3 x 5 pixels centred around the ground pixel of the station, were estimated by the Heliosat procedure from Meteosat image acquisition each half hour for the four stations Lisboa, Lyon, Geneva, and Gävle. For all stations Version 2n together with the Ineichen modification is available, while for Lyon also version 3n is available.

We express the global irradiance in terms of clear sky index, which is the ratio between actual global irradiance (observed or satellite derived) and cloudless global irradiance (Version 2n or 3n). “Percentile match curves” which relate clear sky indices k and cloud indices n are plotted (Fig. 1) as follows: the lowest k against the highest n, the second lowest k against the second highest n, ... the highest k against the lowest n. Such curves (Fig. 1) for the central 95% of the distributions, reveal that Heliosat Version 2n fits nicely for Gävle, in a similar manner as for 9 northern stations (Olseth & Skartveit, 1997). For the three remaining stations the clear sky index vs cloud index relationship tend to be less linear than it is at Gävle, and Version 2n overestimates the clear sky index at intermediate cloud indices. The Ineichen modification of Version 2n yields a better overall performance (except at Gävle), but moves the clear sky mode to a too low value. For Lyon, Version 3n seems to give a better overall performance than does Version 2n.

2.2 Ground truth data

Data from the European General class IDMP stations at Lisboa (38°46'N, 9°08'W, 106 m above m.s.l.; January-November 1994) and Lyon (Vaulx-en-Velin, 45°47'N, 4°56'E, 170 m above m.s.l.; April 1994 - March 1995) were gratefully received from D. Dumortier at ENTPE, Lyon. Besides, data from the Swedish General class station Gävle-Brynäs (60°40'N, 17°10'E, 16 m above m.s.l.; April-November 1995) were gratefully received from H. A. Löfberg at the Royal Institute of Technology, Department of Built Environment, and data from the Research class station at Geneva (46°12'N, 6°06'E, 425 m above m.s.l.; April 1994 - March 1995) were gratefully received from Pierre Ineichen at GAP-Energie, Universite de Geneve.

Global and diffuse horizontal irradiances are measured by Kipp&Zonen CM6 pyranometers at Lisboa and Lyon, and by Kipp&Zonen CM11 pyranometers at Gävle and Geneva. The sensors for diffuse irradiance are shaded with shadow rings in Lisboa (7.7 cm width, 31.5 cm radius), Lyon (5 cm width, 17.8 cm radius),Geneva (8 cm width, 40 cm radius) and with sun tracking shading disk in Gävle (7 cm radius, 70 cm distance). In Geneva normal incidence beam irradiance is also measured by an Eppley NIP.

Horizontal and vertical illuminances are measured by Licor LI-210 SA sensors at Lisboa, by Licor LI-210 SZ sensors at Gävle, and by LMT BAP 30FCT sensors at Lyon. In Geneva global horizontal illuminances and illuminances on vertical surfaces are measured by PRC910GV sensors, while diffuse horizontal illuminance is measured by a Licor sensor. The sensors for horizontal diffuse illuminance are shaded with shadow rings in Lisboa , Lyon, and Geneva (for Lisboa and Geneva these rings have the same dimension as for diffuse irradiances, for Lyon the dimension is: 5.4 cm width, 27.5 cm radius), and with sun tracking shading disk in Gävle (same dimension as for diffuse irradiance). In Geneva, normal beam illuminance is also recorded, using aLicor sensor with tube.

Ground reflected radiation is screened off from the vertical sensors by a black screen (honeycomb). The data used in this paper are hourly values at Lisboa and Gävle, instantaneous values at Lyon, and ten minute averages (± 5 min around the hours of Meteosat data) for Geneva.

3. MODELS

3.1 The luminous efficacy model

The luminous efficacy model (Olseth & Skartveit, 1989) is based on the CIE curve for photopic vision and spectral irradiances obtained by an interpolation between transmittance models for, respectively, cloudless sky (Bird & Riordan, 1986) and unbroken cloud cover (Stephens et al, 1984). This interpolation decomposes the diffuse irradiance into "blue sky", "dark cloud", and "bright cloud" irradiance. For partly cloudy cases, the model was slightly tuned to hourly global illuminance and irradiance from Bergen. The parameterized version of the model requires solar elevation, day of year, and diffuse and beam clearness indices as input. In the case of beam irradiation, the model is slightly modified here to explicitly account for variation in column amount of water vapor, under the assumption that water vapor extinction takes place solely at non-visible wavelengths. Moreover, in the case of diffuse irradiation the model is tuned to data from Albany, NY (gratefully received from R. Perez) by multiplying the difference between "dark cloud" efficacy and extraterrestrial efficacy by a factor 0.7. For Lisboa, Lyon, and Geneva the luminous efficacy model is run with the climatological average monthly water vapor amounts (WMO, 1982). Since Gävle and Bergen are at the same latitude, the model is run with the same monthly watervapor amounts as those estimated for Bergen (0.8-1.9 cm).

3.2 The slope algorithm

Given horizontal beam irradiance/illuminance, the beam irradiance/illuminance on a given slope is readily computed. To calculate the diffuse slope irradiance/illuminance requires additional information about surface reflectance and the horizontal diffuse sky irradiance/illuminance and its angular distribution.

We apply our slope algorithm (Skartveit & Olseth, 1986) for diffuse irradiance even for diffuse illuminance. This algorithm assumes Lambertian ground reflectance and may account for local horizon effects. Sky radiance anisotropy for cloudless as well as overcast skies is parameterized as follows: One fraction, equal to the beam transmittance, of the horizontal diffuse irradiance is treated as circumsolar radiation (Hay, 1979). Another fraction, decreasing from 0.3 at overcast to zero at beam transmittance

= 0.15, is treated as collimated radiation from the zenith. The remaining horizontal diffuse irradiance is treated as isotropic sky radiance.

4. MODELLED VERSUS OBSERVED ILLUMINANCE.

"Modelled" horizontal diffuse/beam illuminance is obtained by transforming observed horizontal diffuse/beam irradiance into illuminance by the luminous efficacy model (Olseth & Skartveit, 1989 - with the above modifications). "Modelled" vertical illuminance is obtained by first transforming observed horizontal diffuse/beam irradiance into slope irradiance using the slope algorithm (Skartveit & Olseth, 1986). This slope irradiance is subsequently transformed into slope illuminance by the luminous efficacy model under the assumption that all components of the diffuse irradiance have the same luminous efficacy as the bulk horizontal diffuse sky irradiance.

With horizontal irradiances (observed at surface) as model input there is a nice agreement between modelled and observed horizontal illuminances, as exemplified for Lisboa and Lyon in Fig. 2a. At the four stations Gävle, Geneva, Lyon and Lisboa, the model vs observed mean bias deviations (for global, beam and diffuse) are in the range $\pm$5% of the corresponding global illuminance (Table 1).

With surface based irradiances as input, the overall average modelled vertical illuminances are lower than the observed ones (Fig. 2b-c, left) for foreground albedo A = 0.0, while this model deficit is almost completely removed by using A = 0.1 (Fig. 2b-c, right). As an average for the four verticals and for the four stations, the model vs observed mean bias deviation are -6.0% of the global illuminance for A=0.0, and -0.3% for A=0.1 (Table 1). It is thus indicated that the horizontal foreground (honeycomb) of the vertical sensors is more close to having A = 0.1 than to being completely black (A = 0.0). In fact, this is exactly the same conclusion as drawn previously from data from Gävle and Geneva (Olseth & Skartveit, 1996, Skartveit & Olseth, 1997). We therefore use foreground Lambertian albedo A = 0.1 for slope calculations in the following.

Both for horizontal and vertical surfaces, the scatter (model vs observed) not unexpectedly increases substantially when the model input is changed from observed horizontal irradiances to global irradiance derived from Meteosat, as exemplified for Gävle and Geneva in Figs. 3,4.

Table 1 shows that, among the four stations, the average global illuminance modelled from half-hourly horizontal irradiances, range from 4.5% lower than observed at Gävle to 2.6% higher than observed at Lyon. For foreground albedo A = 0.1 the modelled average illuminance on the average vertical surface (N-E-W-S average) range from -1.4% (percentage of global illuminance) lower than observed at Geneva to 1.6% higher than observed at Lisboa.

Similarly, the average global illuminance modelled from half-hourly Heliosat Version 2n irradiance range, from 2.9% lower than observed at Gävle to 14.8% higher than observed at Lyon. For foreground albedo A = 0.1 the modelled average illuminance on the N-E-S-W average vertical surface range from 0.1% lower than observed at Gävle to 6.5% higher than observed at Geneva (percentages of global illuminance).

Finally, the average global illuminance modelled from half-hourly Helisoat Version 2n (with the adjustment of Ineichen ,1997) irradiance, range from 11.4% lower than observed at Gävle to 3.7% higher than observed at Lyon. For foreground albedo 0.1 the modelled average illuminance on the N-E-S-W average vertical surface range from -3.8% lower than observed at Gävle to 3.3% higher than observed at Geneva (percentages of global illuminance).

For each of the four stations, Fig. 5 shows “percentile match curves” which relate observed and modelled illuminances (global, beam, horizontal diffuse, and north/east/south/west vertical). These curves are formed by making separate rankings of the half-hourly modelled and observed illuminances. Then each modelled half-hourly illuminance is plotted against the observed half-hourly illuminance which has the same rank number as this modelled value. A reasonable agreement between observed and modelled distributions is seen, and the systematic deviations observed are in agreement with those inferred from Table 1. Moreover, note that the modelled vs observed mean bias deviations, expressed as percentages of the respective global illuminance in Table1, are plotted in terms of klux against their observed counterparts in Fig. 6.

5. CONCLUDING REMARKS

For a horizontal surface, we find at 4 IDMP stations (Gävle, Geneva, Lyon, and Lisboa) a nice conformity between observed half-hourly illuminances (global, beam and diffuse) and illuminances modelled from corresponding horizontal irradiances, with mean bias deviations in the range ±5% of global illuminance.

The horizontal foreground seen by the vertical sensors appears at all four stations to have Lambertian albedo approximately equal to 0.1 rather than equal to 0.0.

When the model input is changed from observed horizontal irradiances to Heliosat global irradiance, the scatter and mean bias deviations (model vs observed) not unexpectedly increases significantly both for horizontal and vertical surfaces.

Judged from mean bias deviations, Helisoat Version 2n fits the Gävle data nicely, while it tends to yield illuminances exceeding the observed ones at Geneva, Lyon and Lisboa. The adjustment proposed by Ineichen (1997), improves the overall performance of Version 2n at Geneva, Lyon and Lisboa, while the opposite is the case at Gävle.

A reasonably conformity is seen between distributions of, respectively, observed and modelled half-hourly illuminances.

6. REFERENCES

H.G. Beyer, C. Costanzo, and D. Heinemann: Modifications of the Heliosat procedure for irradiance estimates from satellite images. Solar Energy, **56**, 207 - 212 (1996).

R.E. Bird and C. Riordan (1986): Simple solar spectral model for direct and diffuse irradiance on horizontal and tilted planes at the earth's surface for cloudless atmospheres. J. Climate Appl. Meteor., **25**, 87.

J.E. Hay (1979): Study of shortwave radiation on non-horizontal surfaces. Report No 79-12, Atmospheric Environment Service, Downsview, Ontario

A. Hammer: Satellite-derived global radiation data kindly submitted (spring 1997).

P. Ineichen: Personal communication (1997).

J.A. Olseth and A. Skartveit (1989): Observed and modelled luminous efficacies under arbitrary cloudiness. Solar Energy, **42**, 221-233.

J.A. Olseth and A. Skartveit (1997): High latitude global and diffuse radiation estimated from METEOSAT data.

A. Skartveit and J.A. Olseth (1986): Modelling slope irradiance at high latitudes. Solar Energy, **36**, 333-344.

A. Skartveit and J.A. Olseth (1994): Luminous efficacy models and their application for calculation of photosynthetically active radiation. Solar Energy,**52**, 391-399.

A. Skartveit and J.A. Olseth (1996): Illuminance/irradiance at a high latitude IDMP station. Second SATELLIGHT meeting, Bergen June 24-25, 1996.

A. Skartveit and J.A. Olseth (1997): Horizontal and vertical illuminance/irradiance from the IDMP station in Geneva. First draft prepared for the third SATELLIGHT meeting, Les Marecotte January 16-17, 1997.

G.L. Stephens, S. Ackerman and E.A. Smith (1984): A short-wave parameterization revised to improve cloud absorption. J. Atmos. Sci., **41**, 687.

World Meteorological Organization (1982): Climatological normals (CLINO) for climate and climate ship stations for the period 1931-1960. WMO/OMM-No.117.

Table 1a) Average observed (Obs) illuminances on north- (N90), east- (E90), south- (S90), west- (W90) facing vertical surfaces, together with the average for all four vertical surfaces (All vertical), and for an horizontal surface (Global, Beam, Diffuse) for Lisboa. Mean Bias Deviation (Mod-Obs), expressed as percentages of average global illuminance is given, for modelled values using irradiances from surface (Surface), from Heliosat Version 2n (V2n), and from the Ineichen modification of Version 2n (V2n+Ineichen) as input. For surface based input both foreground [horizontal] albedo A=0.0 and A=0.1 is used.

		(Mod-Obs)/Glo (%)			
Model input		**Surface**		**V2n**	**V2n+ Ineichen**
Target	**Obs (klux)**	**A=0.0**	**A=0.1**	**A=0.1**	**A=0.1**
N90	**8.1**	**-2.8**	**3.0**	**3.2**	**1.2**
E90	**28.8**	**-5.6**	**0.2**	**3.0**	**-2.5**
S90	**38.1**	**-4.9**	**0.9**	**3.0**	**-3.5**
W90	**16.9**	**-3.3**	**2.5**	**3.3**	**0.0**
All vertical	**23.0**	**-4.2**	**1.6**	**3.1**	**-1.2**
Global	**57.1**	**1.2**	**1.2**	**6.1**	**-5.8**
Beam	**36.9**	**-0.5**	**-0.5**	**2.8**	**-1.1**
Diffuse	**20.2**	**1.6**	**1.6**	**3.3**	**-4.8**

Table 1b) Same as Table 1a), but for Lyon. Heliosat Version 3n (V3n) irradiances are also used as input.

		(Mod-Obs)/Glo (%)				
Model input		**Surface**		**V2n**	**V2n+ Ineichen**	**V3n**
Target	**Obs (klux)**	**A=0.0**	**A=0.1**	**A=0.1**	**A=0.1**	**A=0.1**
N90	**8.0**	**-4.0**	**1.7**	**2.8**	**0.6**	**3.4**
E90	**17.3**	**-6.3**	**-0.6**	**4.6**	**0.3**	**1.4**
S90	**23.9**	**-5.7**	**0.0**	**6.0**	**0.6**	**3.4**
W90	**17.8**	**-8.0**	**-2.3**	**3.7**	**-0.6**	**0.3**
All vertical	**16.8**	**-6.1**	**-0.4**	**4.1**	**0.1**	**2.0**
Global	**35.1**	**2.6**	**2.6**	**14.8**	**3.7**	**8.8**
Beam	**15.4**	**5.4**	**5.4**	**14.5**	**11.1**	**6.3**
Diffuse	**19.6**	**-2.3**	**-2.3**	**0.6**	**-7.1**	**2.8**

Table 1c) Same as Table 1a), but for Geneva.

		(Mod-Obs)/Glo (%)			
Model input		**Surface**		**V2n**	**V2n+ Ineichen**
Target	**Obs (klux)**	**A=0.0**	**A=0.1**	**A=0.1**	**A=0.1**
N90	**7.3**	**-5.4**	**0.3**	**4.4**	**2.2**
E90	**13.6**	**-8.2**	**-2.5**	**6.3**	**3.5**
S90	**20.4**	**-7.9**	**-2.2**	**10.5**	**6.0**
W90	**14.8**	**-7.3**	**-1.6**	**4.4**	**1.3**
All vertical	**14.0**	**-7.1**	**-1.4**	**6.5**	**3.3**
Global	**31.5**	**-2.2**	**-2.2**	**12.4**	**2.5**
Beam	**12.6**	**2.5**	**2.5**	**10.2**	**7.9**
Diffuse	**19.0**	**-5.1**	**-5.1**	**1.9**	**-5.7**

Table 1d) Same as Table 1a), but forGävle.

		(Mod-Obs)/Glo (%)			
Model input		**Surface**		**V2n**	**V2n+ Ineichen**
Target	**Obs (klux)**	**A=0.0**	**A=0.1**	**A=0.1**	**A=0.1**
N90	**8.8**	**-3.7**	**2.0**	**3.1**	**1.1**
E90	**17.8**	**-6.1**	**-0.4**	**1.3**	**-2.0**
S90	**32.9**	**-9.5**	**-3.8**	**-3.6**	**-9.0**
W90	**23.5**	**-5.9**	**-0.2**	**-0.7**	**-4.7**
All vertical	**20.8**	**-6.5**	**-0.8**	**-0.1**	**-3.8**
Global	**44.6**	**-4.5**	**-4.5**	**-2.9**	**-11.4**
Beam	**23.6**	**-4.5**	**-4.5**	**-5.8**	**-7.6**
Diffuse	**21.4**	**-0.7**	**-0.7**	**2.2**	**-4.5**

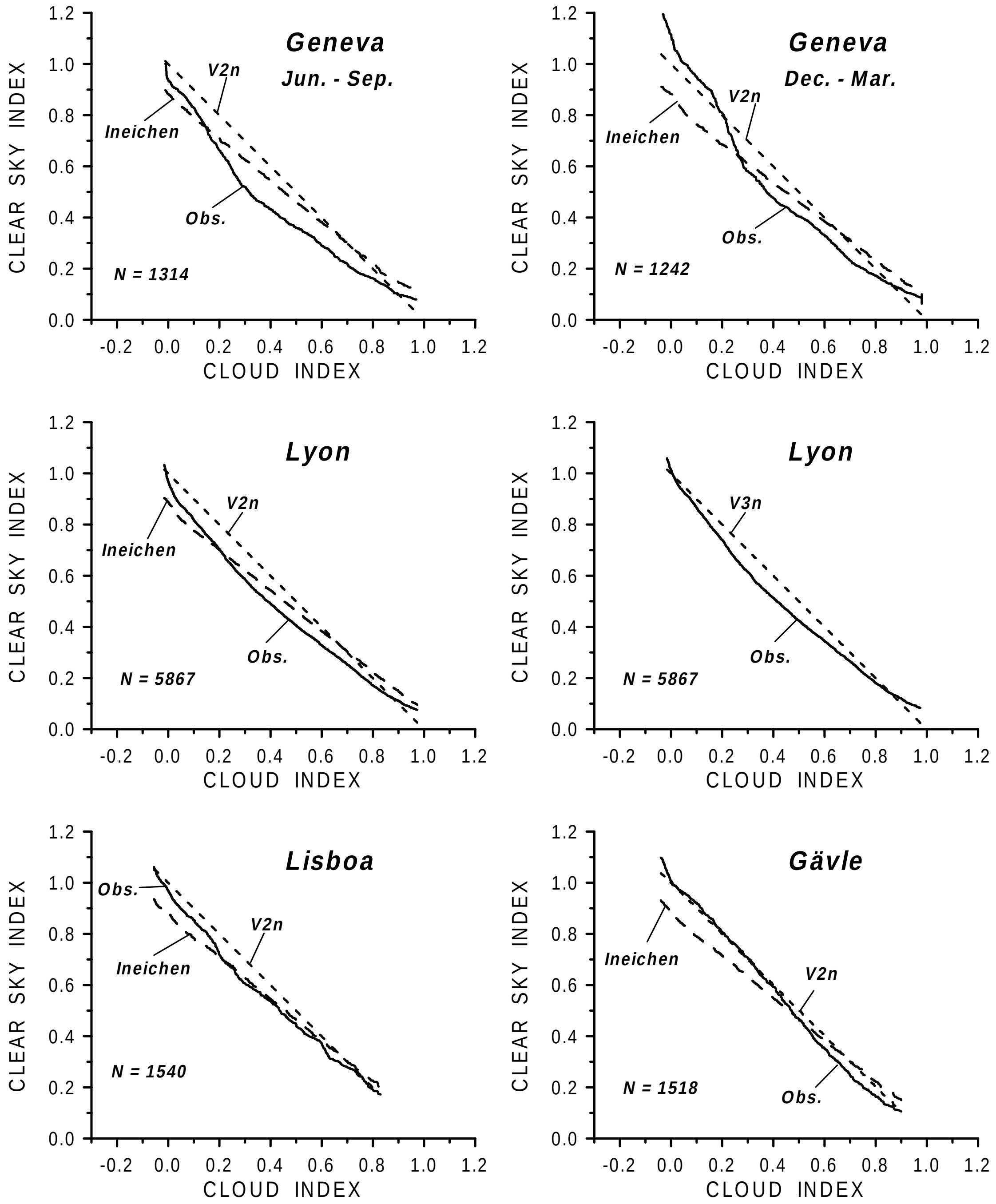

Fig. 1 Upper row: "Percentile match curves" of half-hourly clear sky index (observed and modelled from Heliosat Version 2n and the Ineichen model) and cloud index (modelled from Heliosat Version 2n) [see text] for solar elevation above 10° for the summer (Jun.-Sep., left) and the winter (Dec.-Mar., right) at Geneva. Curves are drawn for the central 95% of the distributions.
Middle row: Similar curves for Lyon for Heliosat Versions 2n (left) and 3n (right).
Lower row: Similar curves for Lisboa and Gävle for Heliosat Version 2n.

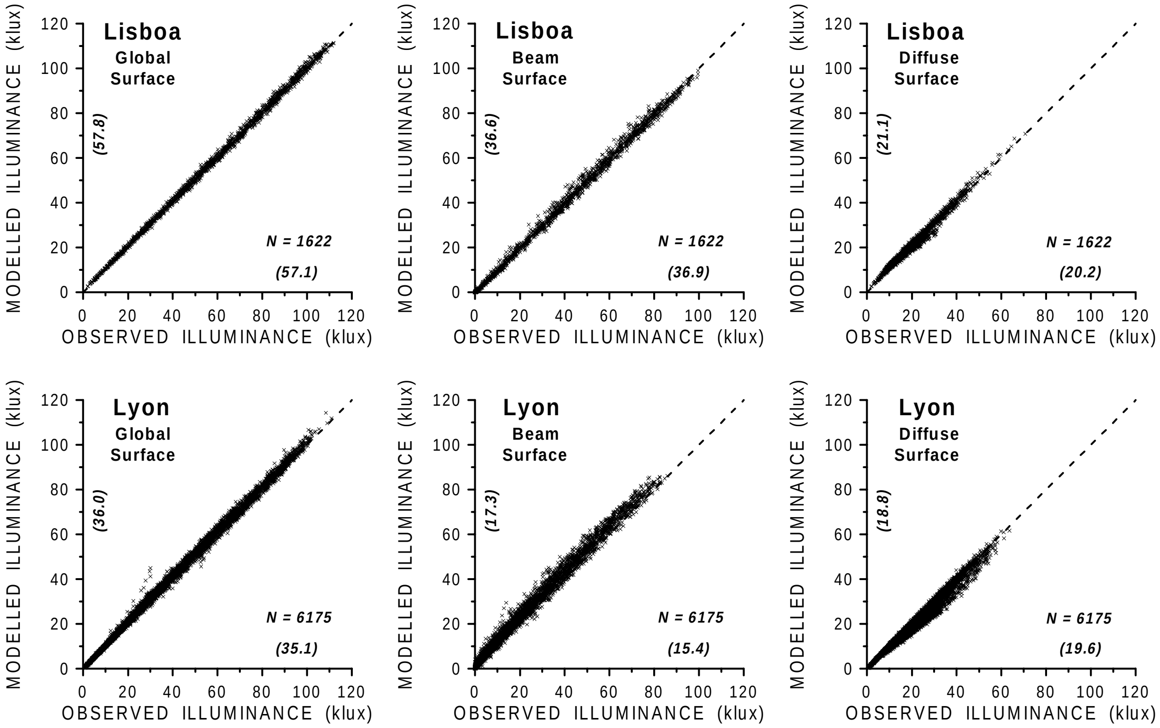

Fig. 2a Observed vs modelled global, beam, and diffuse horizontal illuminances for Lisboa (hourly values) and Lyon (half hourly values). Illuminances are modelled from observed (surface) horizontal irradiances. The number of values (N) are given together with observed and modelled averages (in parentheses along the axes).

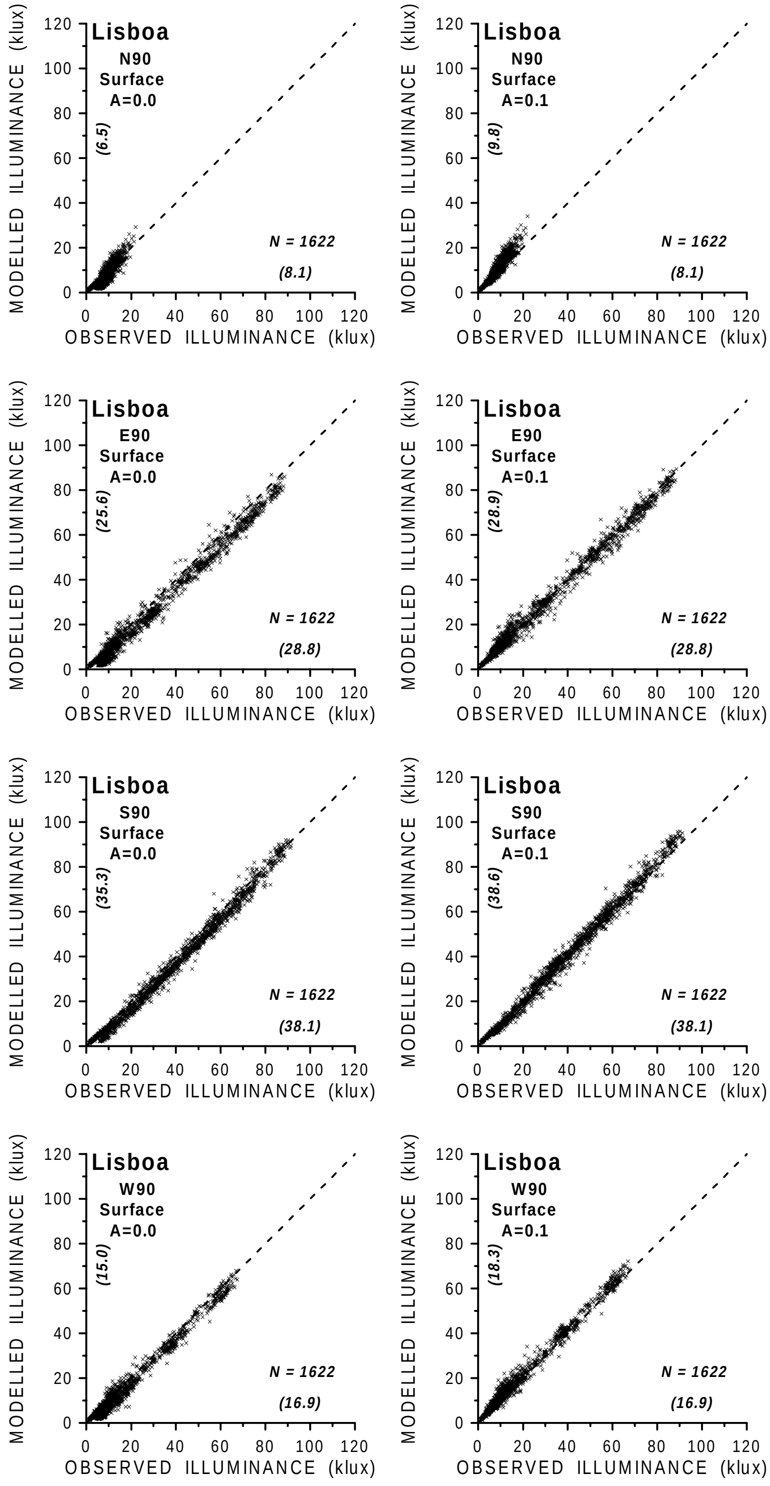

Fig. 2b Observed vs modelled illuminances for vertical surfaces facing north (N90), east (E90), south (S90), and west (W90) for Lisboa (hourly values). Illuminances are modelled from observed (surface) horizontal irradiances using foreground albedo A=0.0 (left column) and A=0.1 (right column). The number of values (N) are given together with observed and modelled averages (in parentheses along the axes).

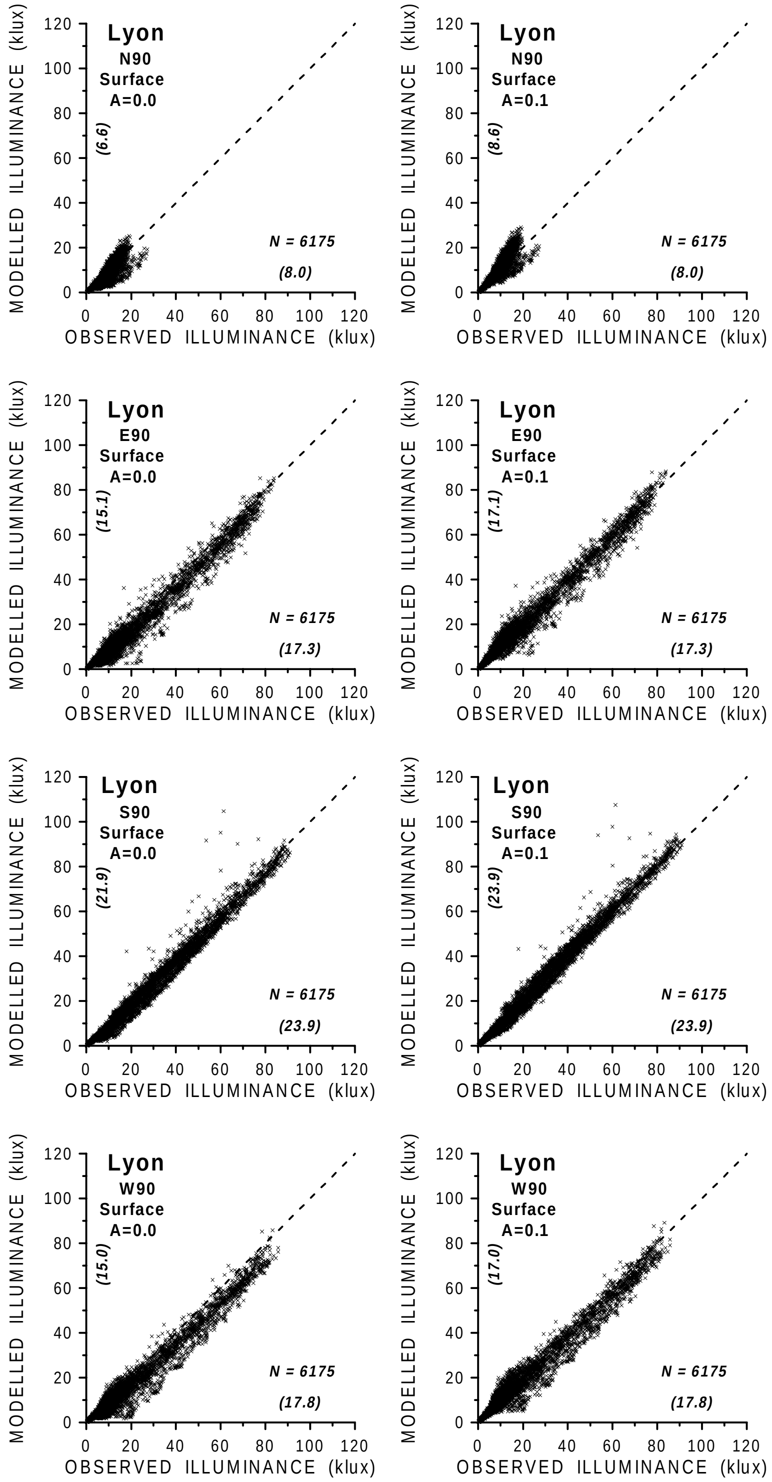

Fig. 2c Same as Fig. 2b, but for Lyon.

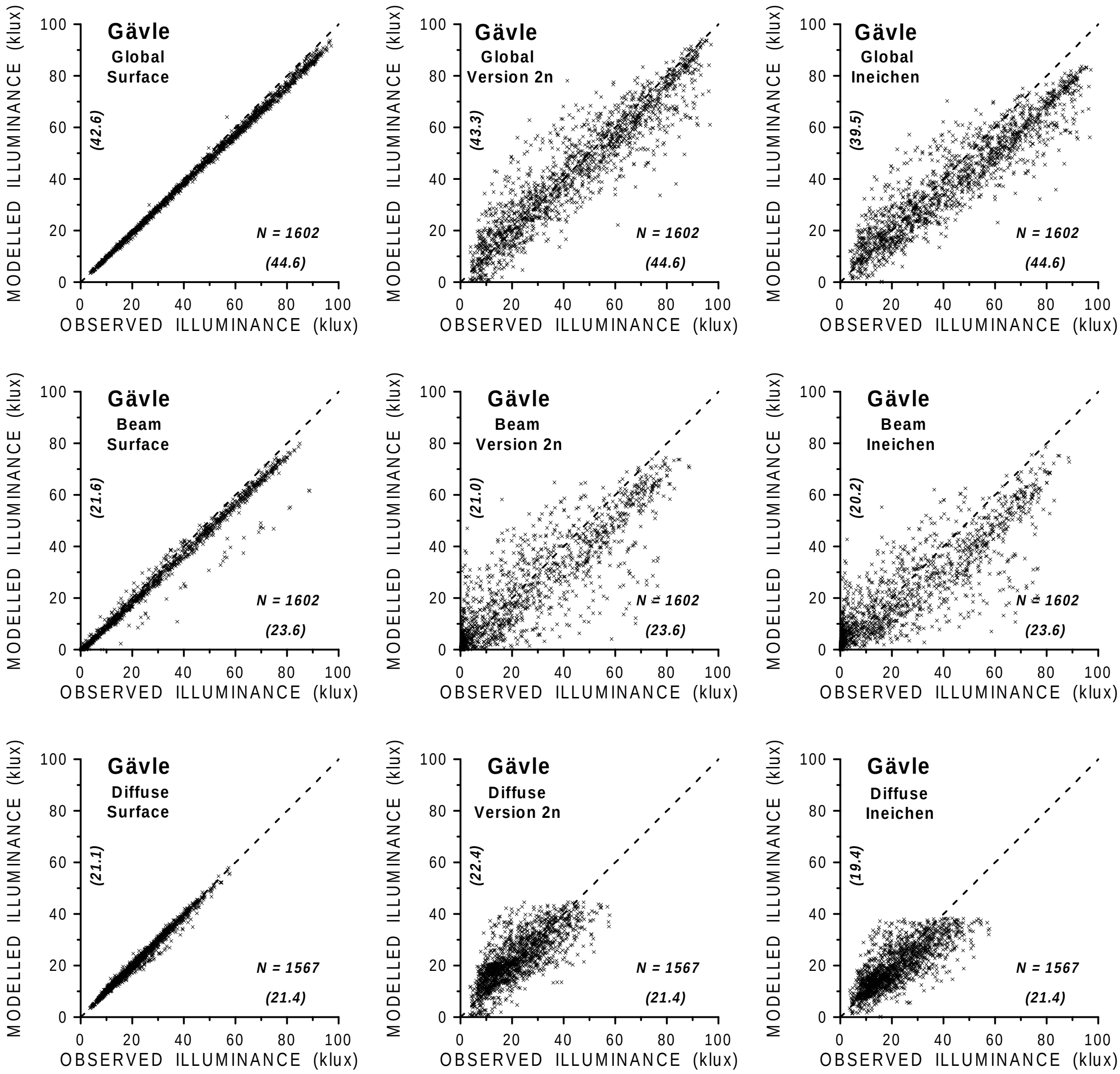

Fig. 3a Observed vs modelled global, beam, and diffuse horizontal illuminances for Gävle. Illuminances are modelled from observed (left column), Heliosat Version 2n (middle column) and Version 2n modified by Ineichen (right column) horizontal irradiances. The number of values (N) are given together with observed and modelled averages (in parentheses along the axes).

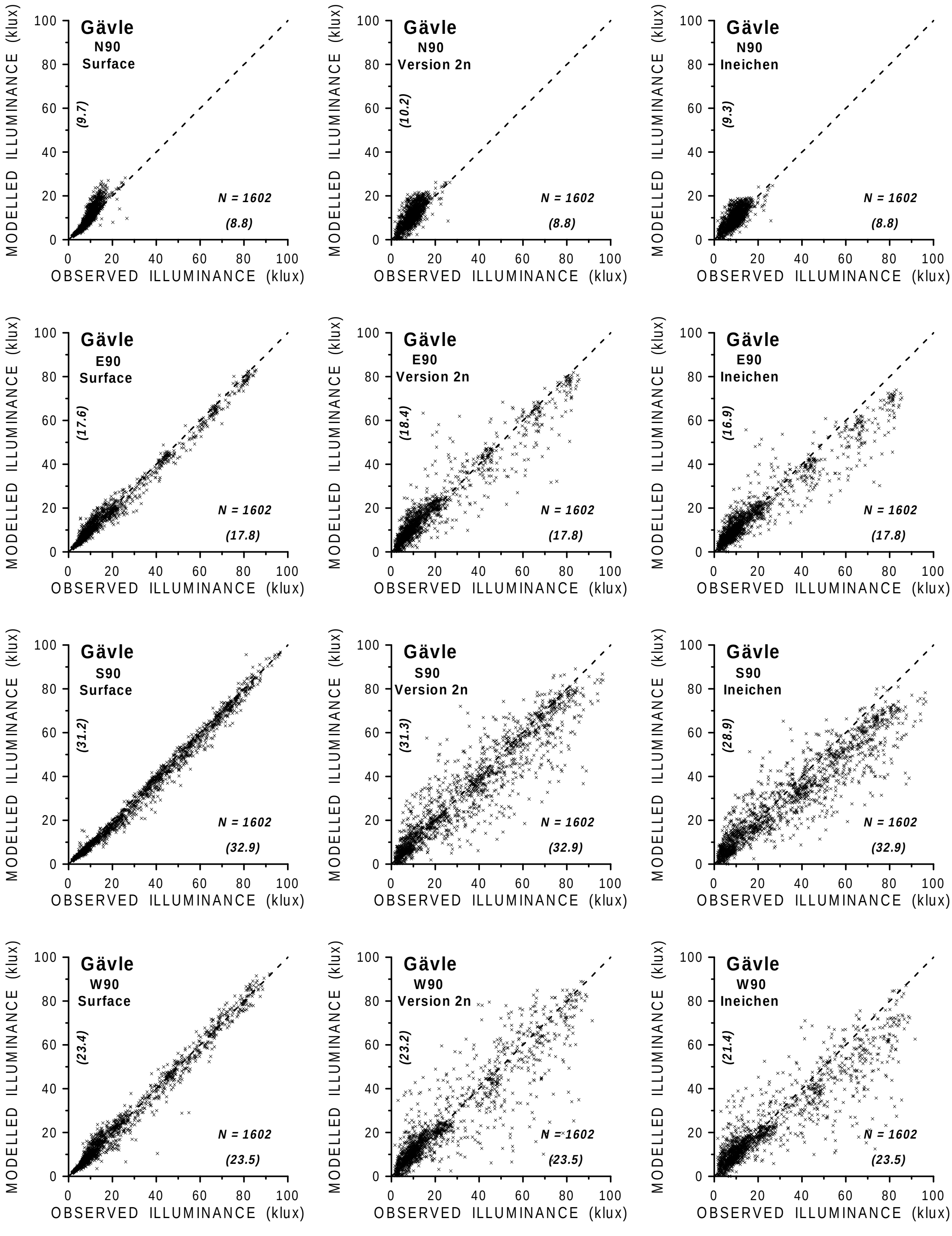

Fig. 3b Same as Fig. 3a, but for vertical surfaces facing north (N90), east (E90), south (S90), and west (W90). Illuminances are modelled from horizontal irradiances using foreground albedo A=0.1.

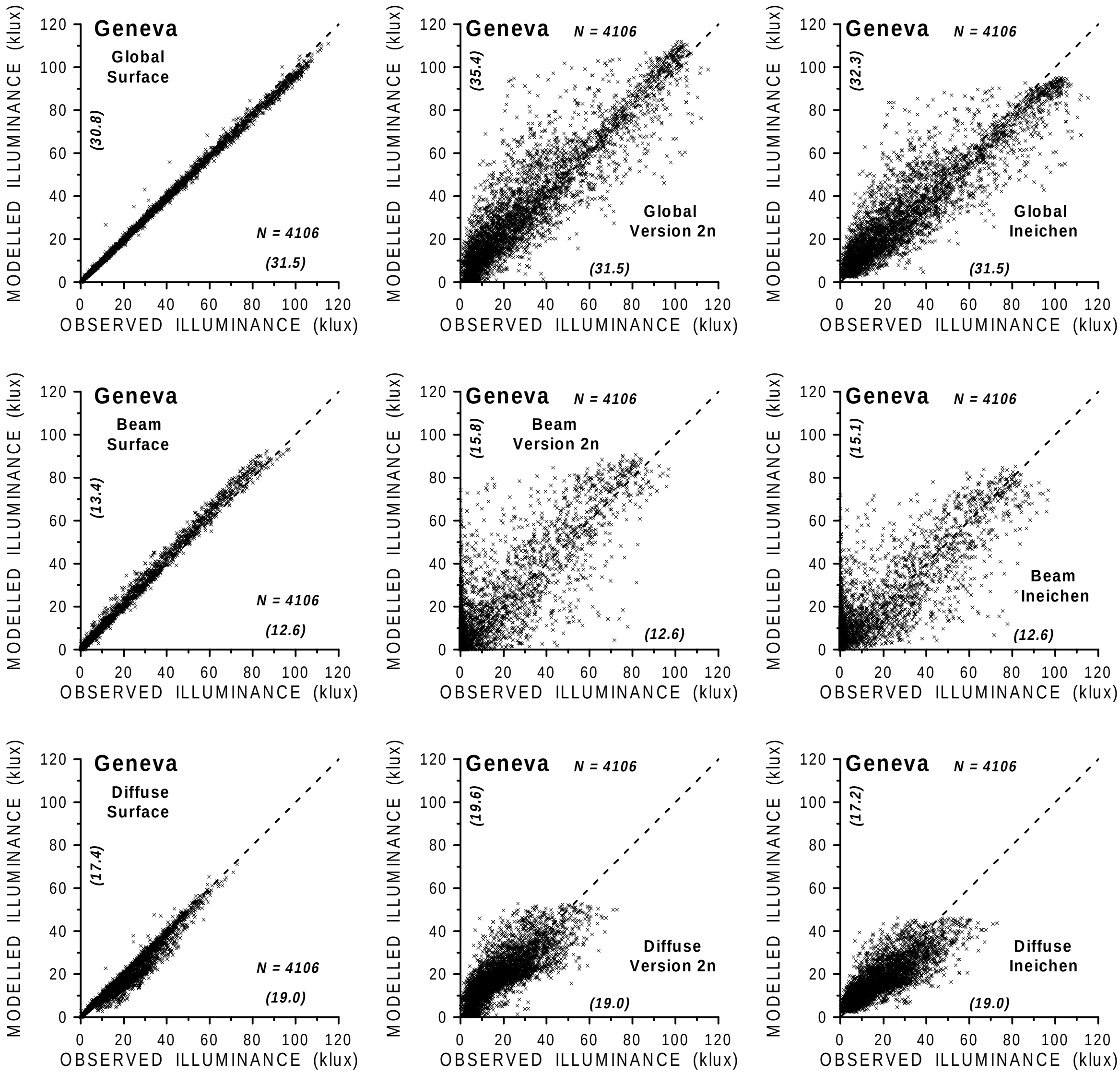

Fig. 4a Same as Fig. 3a, but for Geneva.

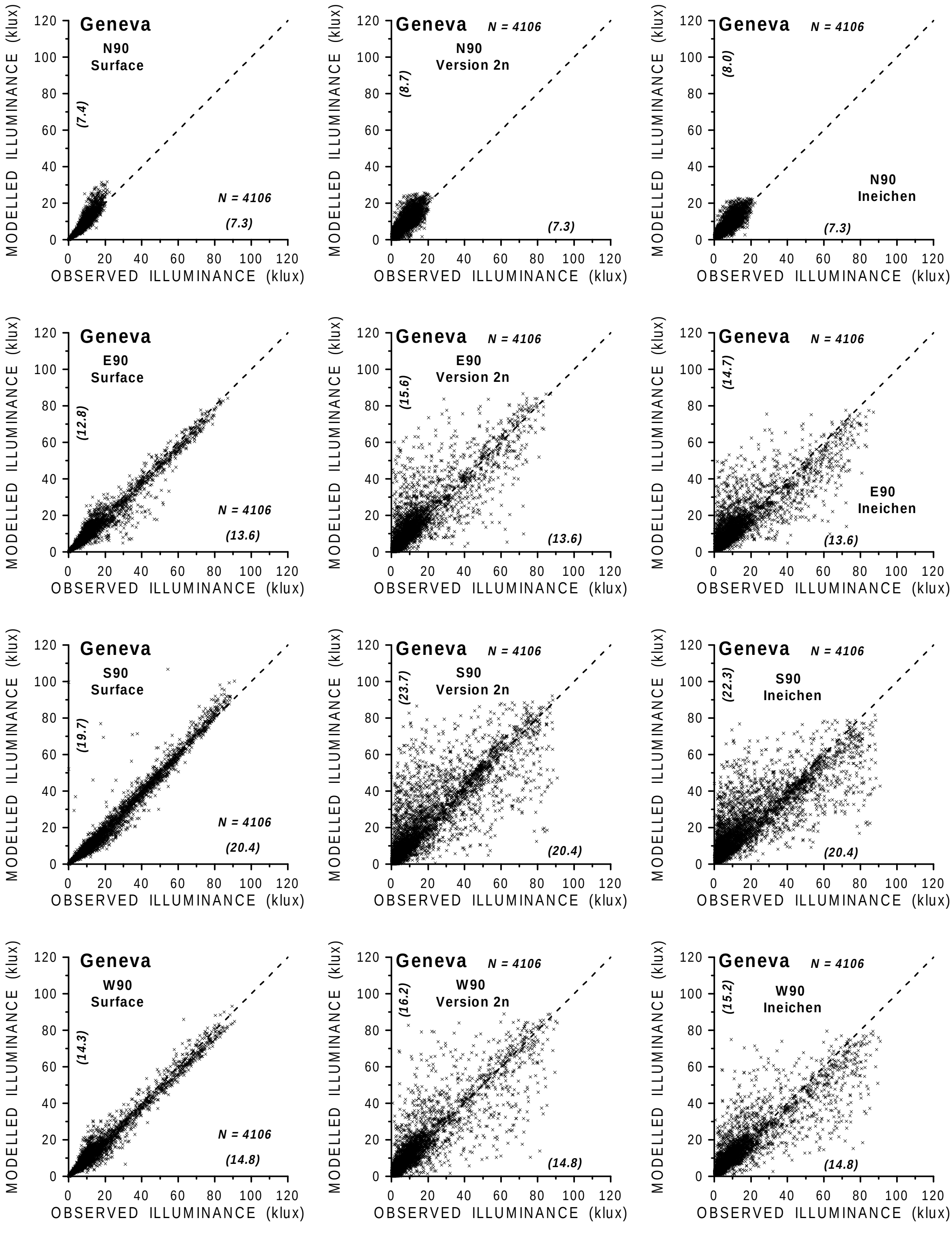

Fig. 4b Same as Fig. 3b, but for Geneva.

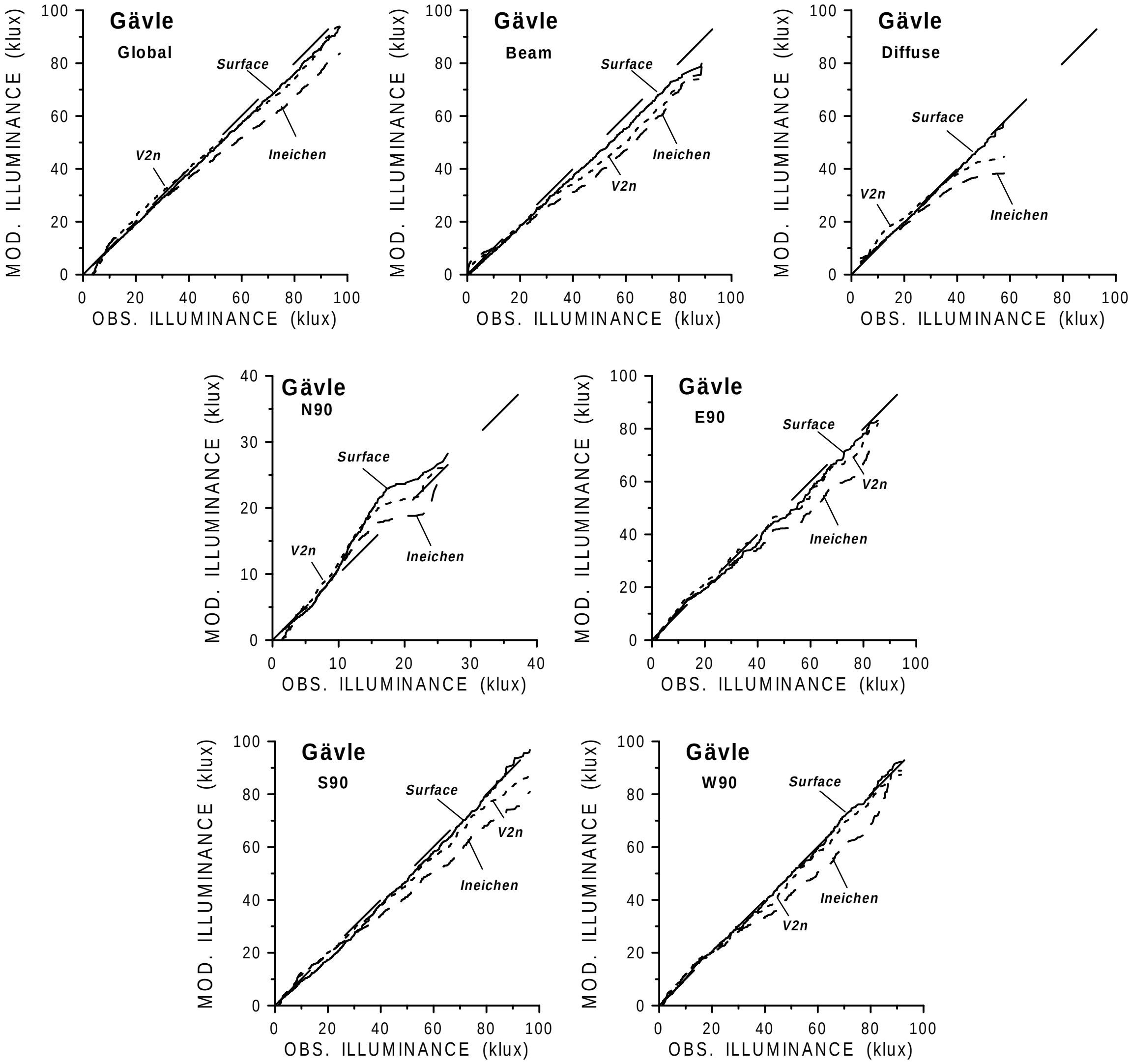

Fig. 5a ″Percentile match curves of observed and modelled global, beam, and horizontal diffuse illuminance (upper row), and illuminances on vertical surfaces facing north (N90), east (E90), south (S90), and west (W90) for Gävle. Illuminances are modelled from observed (surface), Heliosat Version 2n (V2n) and Version 2n modified by Ineichen (Ineichen) horizontal irradiances with foreground albedo A=0.1. The 1 to 1 lines are also given.

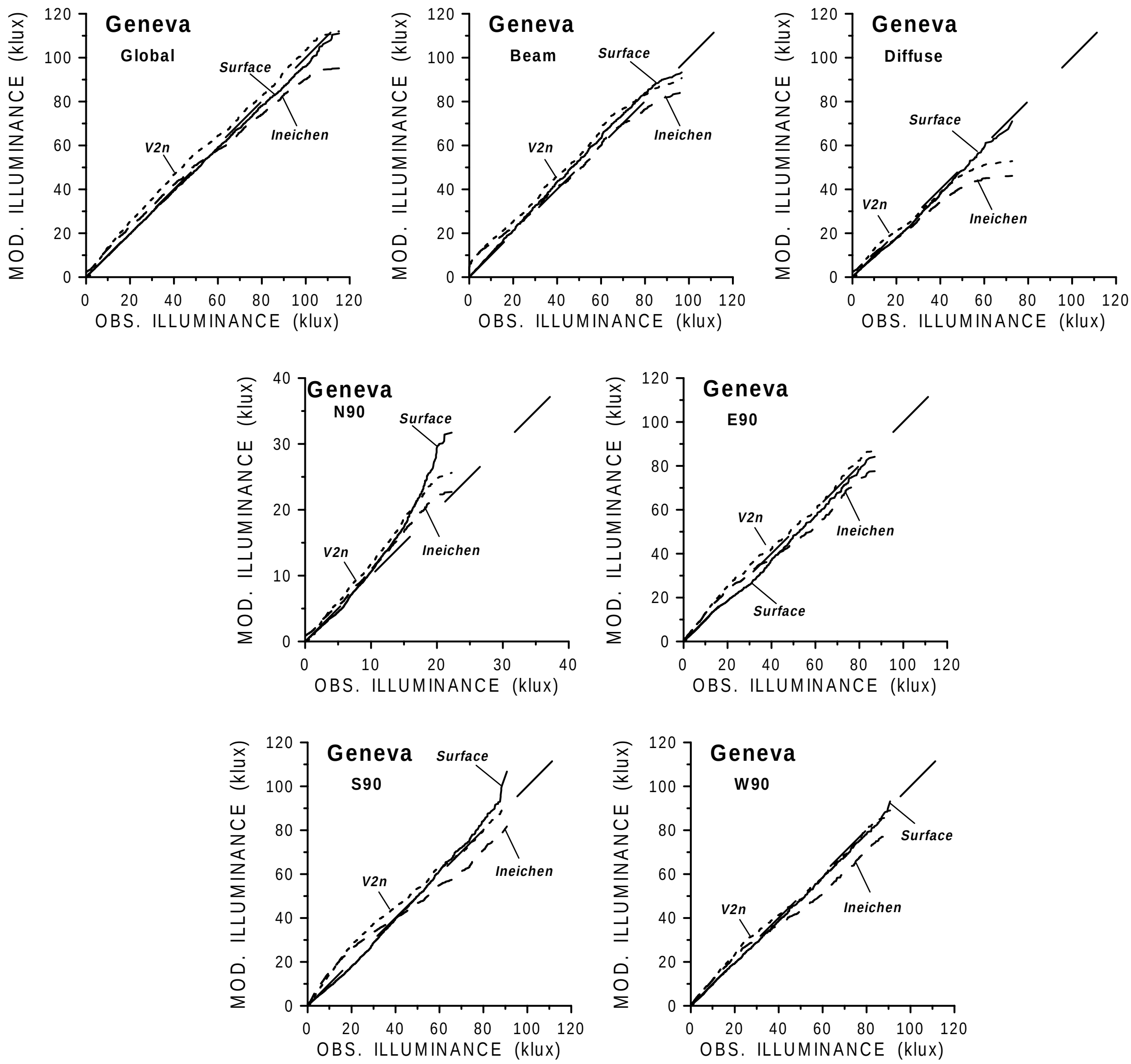

Fig. 5b Same as Fig. 5a, but for Geneva.

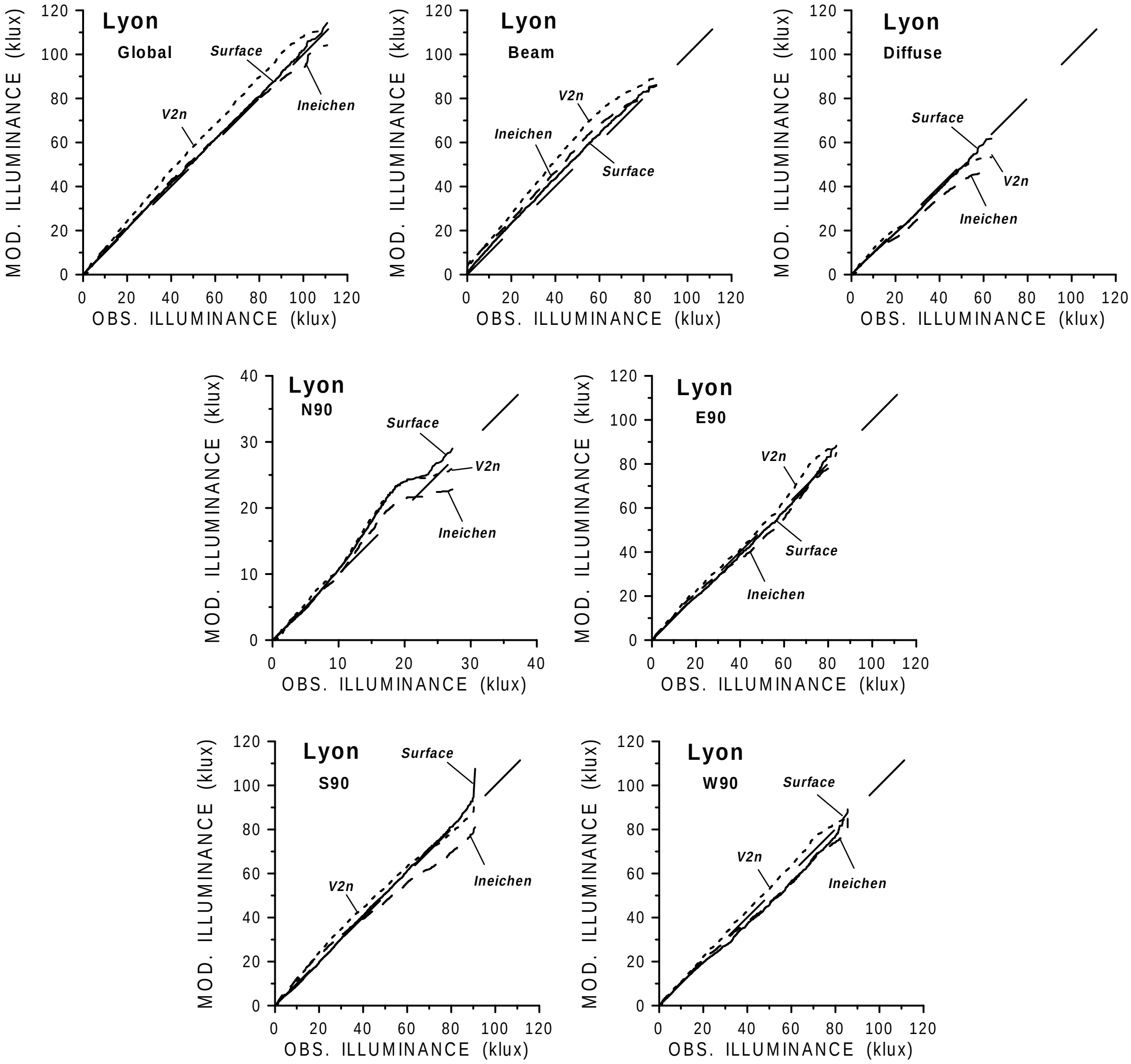

Fig. 5c Same as Fig. 5a, but for Lyon.

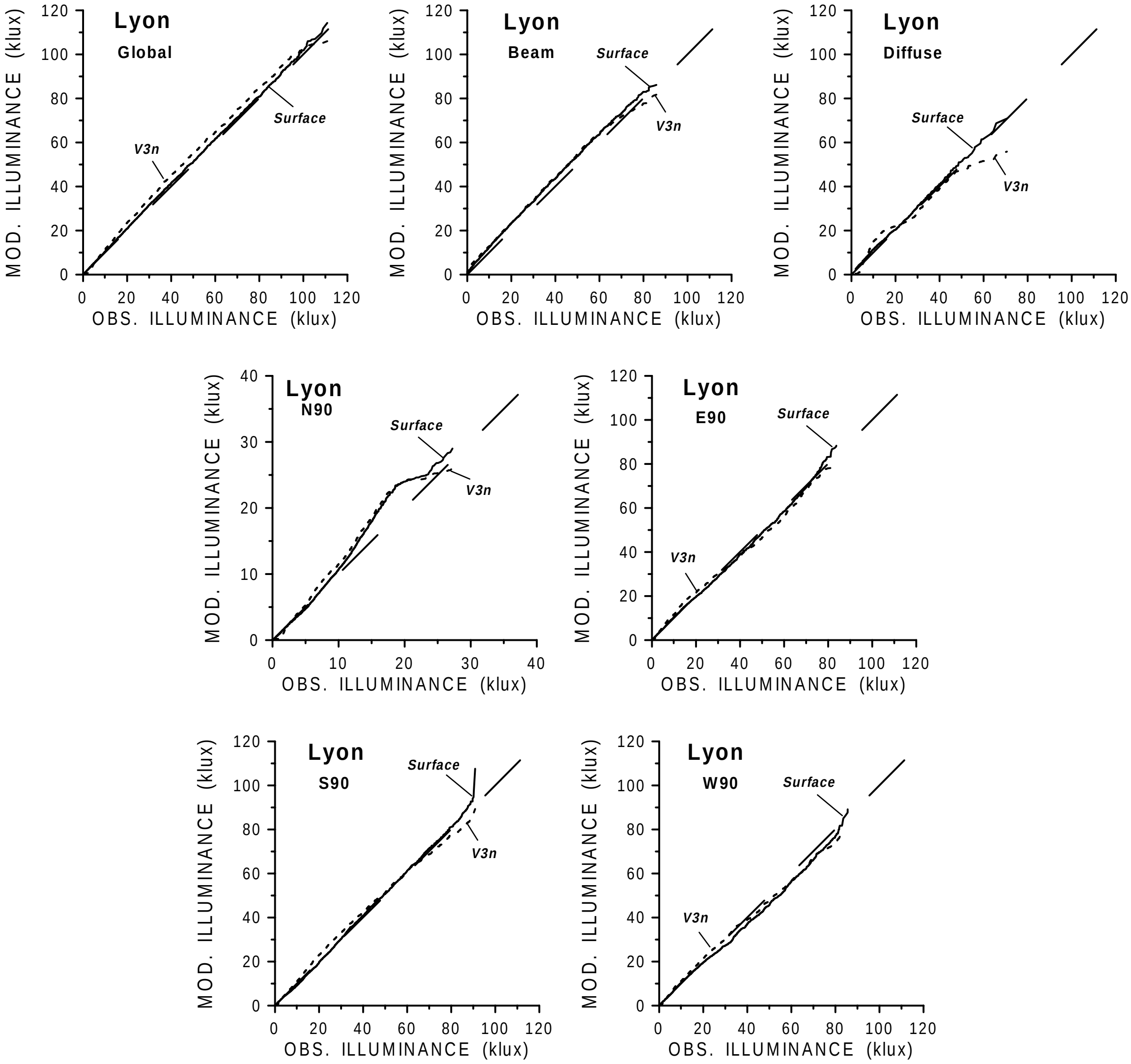

Fig. 5d Same as Fig. 5a but for Lyon., where illuminances are modelled from observed (surface), Heliosat Version 3n (V3n) horizontal irradiances.

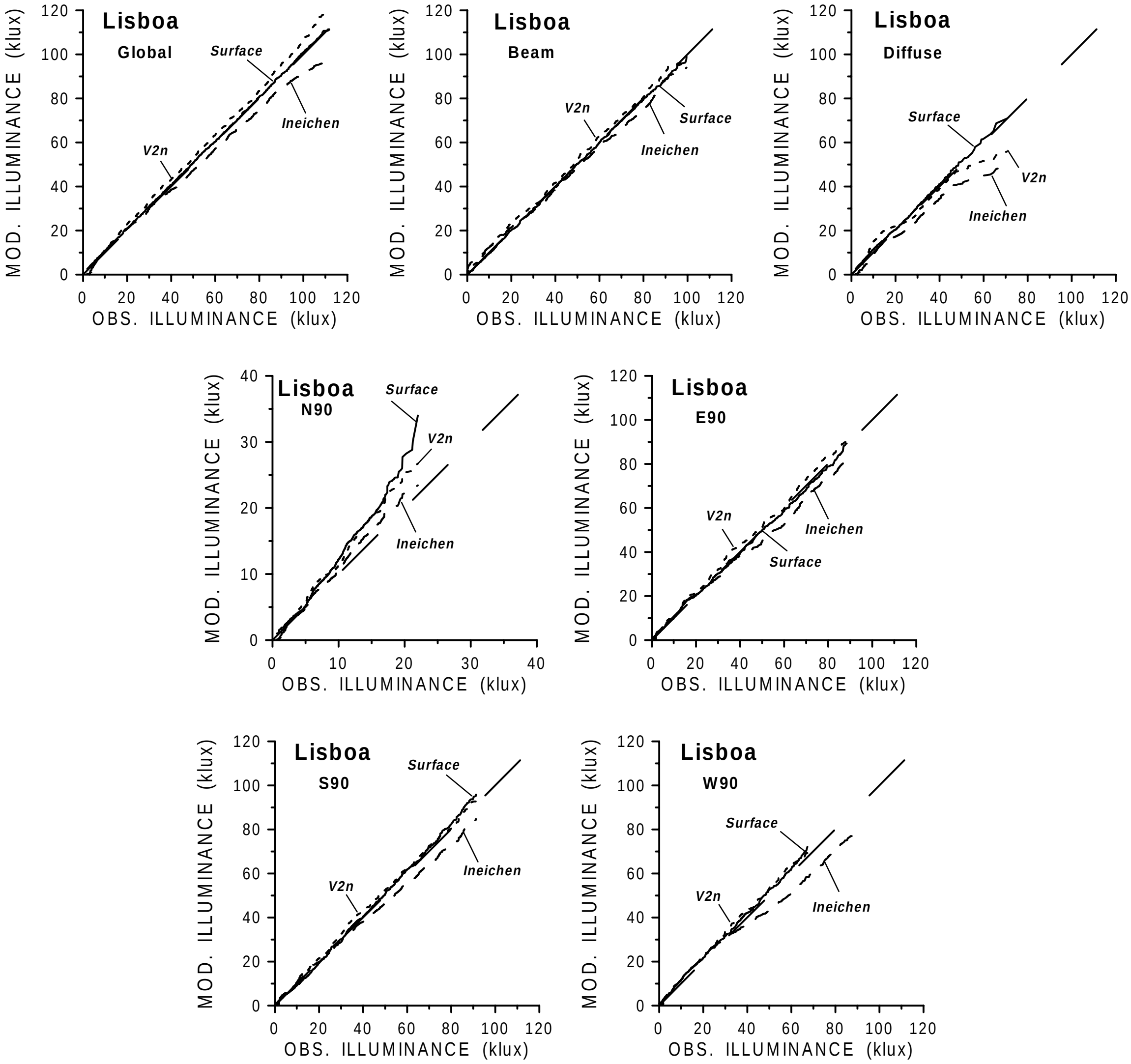

Fig. 5e Same as Fig. 5a, but for Lisboa.

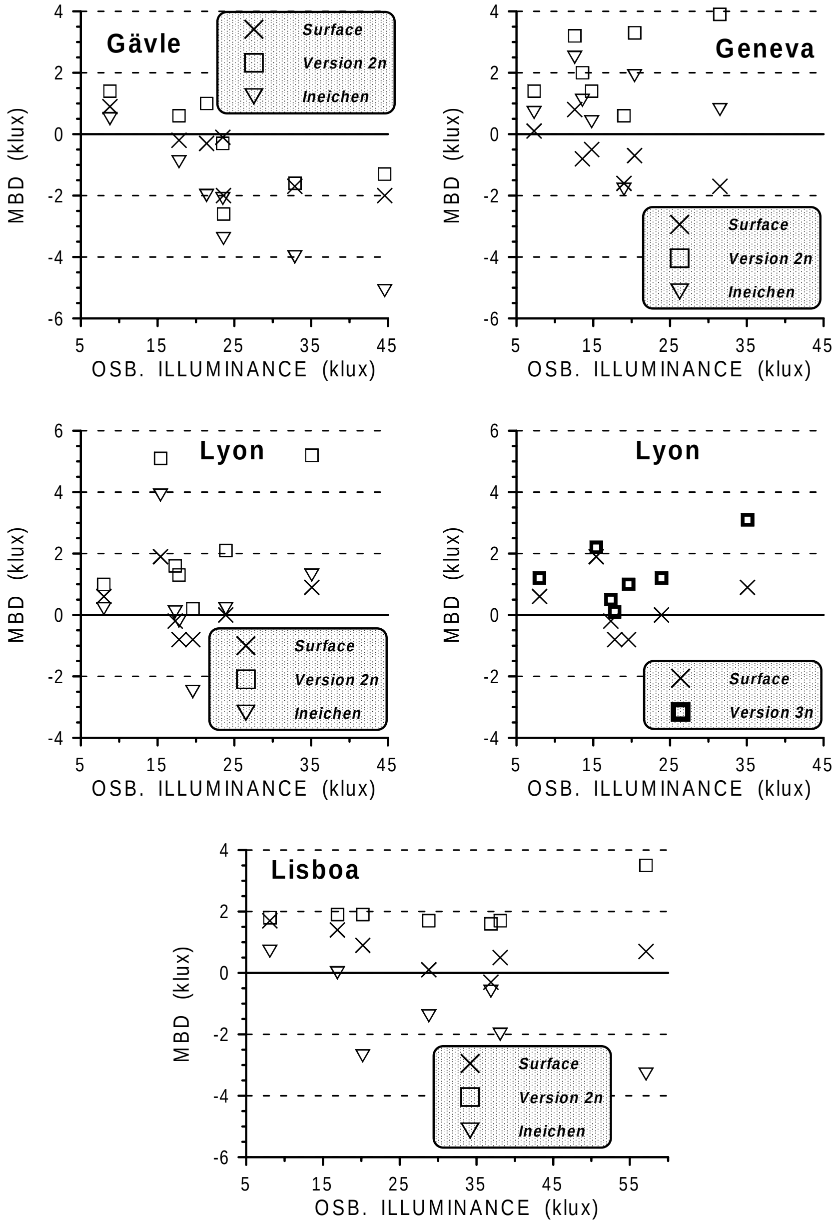

Fig. 6 Mean Bias Deviation (MBD=Modelled-Observed) vs observed illuminance of global, beam, and diffuse horizontal illuminance and illuminances on four vertical surfaces for the four stations. Illuminances are modelled from observed (surface), Heliosat Version 2n (V2n), Version 2n modified by Ineichen (Ineichen), and Heliosat Version 3n (V3n; for Lyon only) horizontal irradiances with foreground albedo A=0.1.